Structure-Based Design, Synthesis, and X-ray Crystallography of a High-Affinity Antagonist of the Grb2-SH2 Domain Containing an Asparagine Mimetic

Pascal Furet,*,† Carlos García-Echeverría,† Brigitte Gay,† Joseph Schoepfer,† Martin Zeller,‡ and Joseph Rahuel§

Oncology Research Department, Novartis Pharma Inc., CH-4002 Basel, Switzerland

Received February 2, 1999

Previous efforts in the search for molecules capable of blocking the associations between the activated tyrosine kinase growth factor receptors and the SH2 domain of Grb2 had resulted in the identification of 3-amino-Z-pTyr-Ac_6c-Asn-NH2, a high-affinity and selective antagonist of this SH2 domain. In the present paper, we report the successful replacement of asparagine in this compound by a β-amino acid mimetic, which brings us closer to our objective of identifying a Grb2-SH2 antagonist suitable for pharmacological investigations.

Introduction

The adapter protein Grb2 is an essential component of the molecular machinery used by tyrosine kinase growth factor receptors to transmit mitogenic signals inside the cell.[1−3] Grb2 contains a Src homology 2 (SH2) domain whose function is to specifically associate with phosphotyrosine (pTyr)-containing motifs present in the intracellular part of the activated receptors. Interruption of the transmission of mitogenic signals in deregulated cancerous cells by chemical blockade of these associations is regarded as a possible strategy to discover new antitumor agents.[4−6] Using the minimal peptide sequence pTyr-Ile-Asn retaining micromolar affinity for the Grb2-SH2 domain as an initial lead structure, we have engaged in a medicinal chemistry effort based on this concept. We recently reported the structure-based design of several modifications imparting high affinity to the minimal sequence.[7−9] In particular, attachment of a 3-aminobenzyloxycarbonyl (Z) N-terminal group combined with replacement of the central isoleucine residue by 1-aminocyclohexane carboxylic acid (Ac_6c) resulted in 3-amino-Z-pTyr-Ac_6c-Asn-NH2 (**1**), a potent (IC_{50} = 1 nM in an ELISA assay) and selective antagonist of the Gbr2-SH2 domain. The high potency of this compound prompted us to undertake additional efforts directed at reducing its peptidic character. Along this line, we present here the design, synthesis, and confirmation of the binding mode by X-ray crystallography of an analogue of **1** in which the Asn residue has been replaced by a nonproteinogenic cyclic β-amino acid mimetic without loss of activity.

Design

The X-ray crystal structure of the Grb2-SH2 domain complexed with the phosphotyrosyl peptide H-Lys-Pro-Phe-pTyr-Val-Asn-Val-NH2 (the 174−180 sequence of the BCR-abl protein) has been determined in our group.[10] This has revealed with full atomic details the structural basis of ligand recognition by the Grb2-SH2 domain. One of the key elements for recognition is the asparagine residue in position pTyr + 2[11] of the sequence of phosphopeptide ligands.[12,13] In the X-ray structure, this asparagine occupies position i + 2 of a type I β-turn allowing the carboxamide group of its side chain to make three specific hydrogen bonds with the peptide backbone of the SH2 domain at residues Lys βD6 and Leu βE4[14] as depicted in Figure 1. Using this structural information, we looked for possible mimetics of asparagine in **1**.

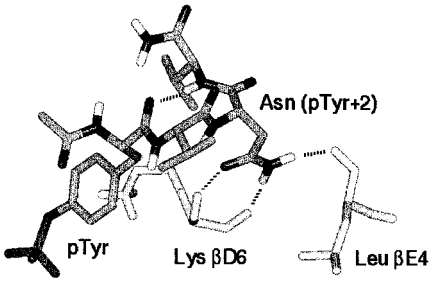

Figure 1. The asparagine of the ligand makes two hydrogen bonds in a bidentate manner with the backbone NH and carbonyl of Lys βD6 and one hydrogen bond with the backbone carbonyl of Leu βE4 (dashed lines). The β-turn intramolecular hydrogen bond between the NH of residue pTyr + 3 and the backbone carbonyl of pTyr is also represented. For clarity, the residues of the ligand N-terminal to pTyr are not shown.

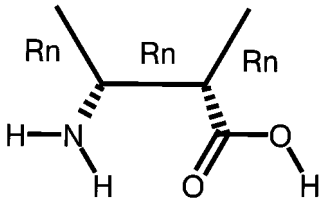

Figure 2. Substructure query used in the database search. Rn means bond belonging to a ring.

The C-terminal carboxamide group of **1** corresponds to the peptide bond connecting residues Asn (pTyr + 2) and Val (pTyr + 3) in the phosphopeptide of the X-ray structure. Inspection of the latter shows that this amide bond has no interactions with the SH2 domain. However, its NH group is involved in the intramolecular hydrogen bond with the backbone carbonyl of the phosphotyrosine residue that stabilizes the β-turn conformation. Deletion of this carboxamide group in **1** by

* Corresponding author. E-mail: pascal.furet@pharma.novartis.com.
The authors contributed equally to the reported work.
† Oncology Research.
‡ Novartis CropProtection
§ Core Technology Area.

10.1021/jm991013u CCC: $18.00 © 1999 American Chemical Society
Published on Web 06/09/1999

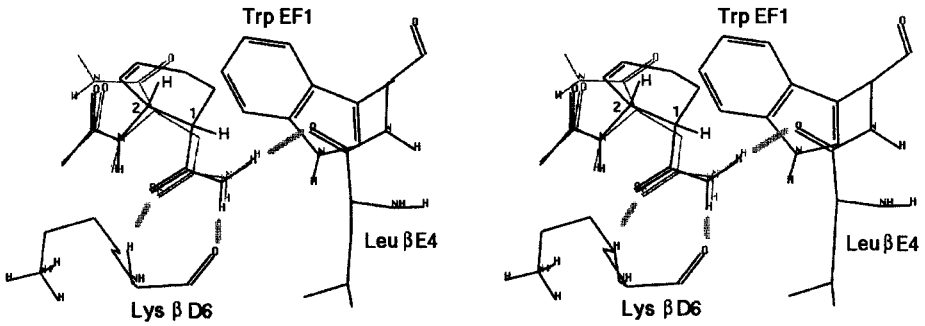

Figure 3. Designed cyclic β-amino acid mimetic (black) of the asparagine moiety (gray). Hydrogen bonds are shown as thick lines (stereoview).

replacement of Asn by β-alanine, leading to a molecule which retains the capacity to make the same hydrogen bonds as with the side chain of asparagine but lacking the C-terminal carboxamide group, resulted in a dramatic loss of affinity for the Grb2-SH2 domain.[15] This result suggested the importance of introducing conformational restriction in potential mimetics of the asparagine moiety.

Interactive modeling based on the X-ray structure showed that it was possible to construct a ring connecting the α and β carbons of the phosphopeptide asparagine while preserving the orientation of the side chain carboxamide necessary to form the three hydrogen bonds. In addition, the ring did not clash with the SH2 domain if it was built in the direction opposite to residue Trp EF1 of the protein. This led to the idea of replacing asparagine by a cyclic β-amino acid, providing rigidity. Following this direction, a substructure search in the chemical archives of the company based on the query shown in Figure 2 was performed. The search returned *cis*-2-amino-cyclohex-3-ene carboxylic acid (*cis*-Achec) as an available six-membered ring β-amino acid synthesized in an unrelated project. Molecular modeling confirmed the suitability of this amino acid as a substitute for asparagine. As shown in Figure 3, *cis*-Achec-NH2 constructed as the (1*S*,2*R*) enantiomer in a half-chair conformation with equatorial and axial positions for the amino and carboxy groups, respectively, can adequately mimic the asparagine of the ligand in its interactions with the SH2 domain. Thus, Asn in **1** was replaced by *cis*-Achec resulting in compounds **2a** and **2b**. Although still able to form the three hydrogen bonds with Lys βD6 and Leu βE4, the compound containing the (1*R*,2*S*) enantiomer of *cis*-Achec was expected to be less potent due to steric clash of its cyclohexene ring with the SH2 domain residue Trp EF1.

Chemistry and Biology

The cyclic β-amino acid **3** was prepared as depicted in Scheme 1. *rac,cis*-7-Azabyciclo[4.2.0]-oct-4-en-8-one (**4**) was synthesized by known procedures[16] using sodium sulfite for the reduction of the *N*-chlorosulfonyl β-lactam.[17] The cis orientation assigned to the fused β-lactam is that expected for a dipolar addition of chlorosulfonyl isocyanate with olefinic substrates.[17] After protection of the amino functionality with the *tert*-butoxycarbonyl group, the β-lactam was hydrolyzed with lithium hydroxide to afford the N^{β}-Boc protected cyclic β-amino acid **6**. For synthetic reasons, the Boc group was removed under acidic conditions and replaced with the Fmoc group.

Scheme 1[a]

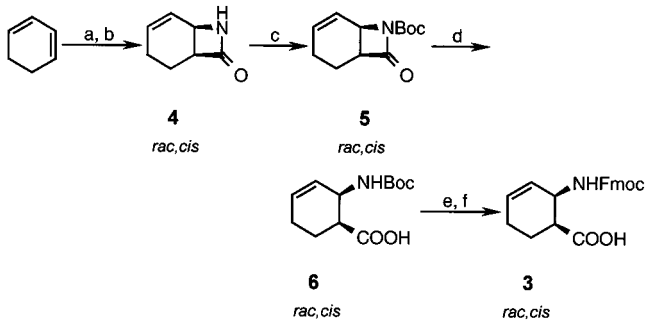

[a] Conditions: (a) $ClSO_2NCO$, DCM; (b) $KCO_3-Na_2SO_3$, 35%; (c) Boc_2O, TEA, DMAP, DCM, 82%; (d) $LiOH\cdot H_2O$, THF/H_2O, 91%; (e) 4 N HCl in dioxane; (f) FmocOSu, TEA, MeCN:H_2O (1:1, v/v), 80%.

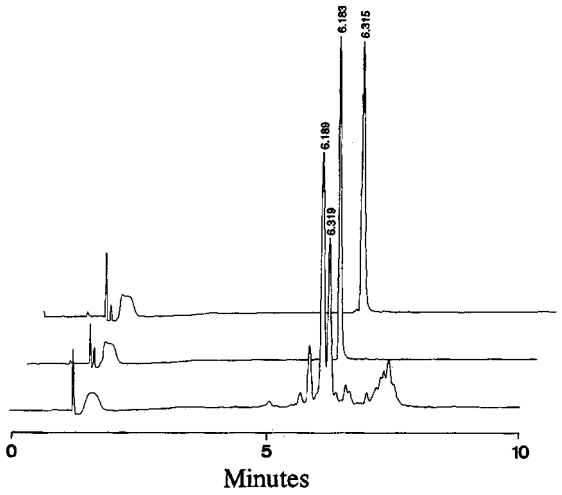

Figure 4. Chromatograms for the separation and purification of compounds **2a** and **2b**.

Compound **2** (3-amino-Z-pTyr-Ac_6c-(cis)-Achec-NH2) was synthesized manually on a Rink amide MBHA resin,[18] employing the Fmoc/*tert*-butyl strategy.[19] The protected cyclic β-amino acid **3** and the required N^{α}-Fmoc-amino acids were incorporated to the solid support using standard coupling protocols. After completion of the synthesis, the peptide resin was simultaneously cleaved and deprotected with 95% TFA−water (19:1, v/v). The HPLC trace of the crude phosphopeptide displayed two main products with identical masses (Figure 4). As expected from the use of the racemic β-amino acid **3**, the two main compounds (**2a** and **2b**) correspond to the two diastereomers of phosphopeptide **2**, which were purified to homogeneity by preparative reversed-phase MPLC (Figure 4).

Table 1. Inhibitory Activity of Compounds **1**, **2a**, and **2b** in EGFR Assay[a]

entry	compound	IC_{50} (nM)
1	3-amino-Z-pTyr-Ac_6c-Asn-NH_2	1.0 ± 0.2
2a	3-amino-Z-pTyr-Ac_6c-(1*R*,2*S*)-Achec-NH_2	>5000
2b	3-amino-Z-pTyr-Ac_6c-(1*S*,2*R*)-Achec-NH_2[b]	1.6 ± 0.1

[a] IC_{50} concentration to inhibit the binding of the phosphorylated C-terminal intracellular domain of EGFR to the Grb2-SH2 domain. Dose−response relationships were constructed by nonlinear regression of the competition curves with GraFit 3.0 (Erithacus Software Limited, London, U.K.). The errors quoted correspond to the standard error in the fits of the data. [b] Stereochemistry assignment based on X-ray structure.

The Grb2-SH2 inhibitory activity of compounds **2a** and **2b** was determined in our EGFR assay (Table 1). This assay measures the potency of a compound to inhibit the binding of the phosphorylated intracellular domain of the epidermal growth factor receptor (EGFR) to the Grb2-SH2 domain. The most potent diastereomer is **2b** which, remarkably, has a binding affinity almost identical to that observed for our reference compound, the asparagine-containing phosphopeptide **1** (IC_{50} = 1.6 nM versus 1.0 nM). In addition, we found that **2b** binds selectively to the SH2 domain of Grb2 as testified by the lack of affinity of the compound for the SH2 domain of $p56^{lck}$, a SH2 domain having a different specificity than that of Grb2 (no inhibition at a concentration of 10 μM in a phosphopeptide competition assay previously described[9]).

The X-ray structure of the Grb2-SH2 domain complexed with compound **2b** allowed the determination of the configuration of the cylic β-amino acid in the highly potent diastereomer.

X-ray Crystallography. The Grb2-SH2 domain was cocrystallized with compound **2b** and the X-ray structure of the complex solved at 3.0 Å resolution. The structure revealed the expected (1*S*,2*R*) configuration of *cis*-2-amino-cyclohex-3-ene carboxylic acid in **2b**. The main interactions of the ligand with the SH2 domain are shown in Figure 5. As can be seen, the asparagine mimetic functions as designed. Its carboxamide moiety forms two hydrogen bonds in a bidentate manner with the backbone carbonyl and NH of Lys βD6 and an additional one with the backbone carbonyl of Leu βE4. Moreover, the structure confirms the validity of earlier design. As predicted, one observes a stacking interaction of the phenyl ring of the 3-amino-Z N-terminal group with the guanidinium moiety of Arg αA2,[7] and Ac_6c adopts a right-handed 3_{10} helical conformation with its side chain making hydrophobic van der Waals contacts with Phe βD5 and Gln βD3.[8] Other important interactions are identical to those seen in the X-ray structure of the Grb2-SH2 domain complexed with the phosphopeptide H-Lys-Pro-Phe-pTyr-Val-Asn-Val-NH2.[10] In particular, the phosphotyrosine binds exactly the same way, its phosphate group forming hydrogen bonds with the side chains of Arg βB5 and Arg αA2. The backbone NH of residue pTyr + 1 is also involved in a hydrogen bond with the backbone carbonyl of His βD4.

Conclusion

In phosphotyrosyl peptides, specificity for binding to the SH2 domain of Grb2 is determined by the presence of asparagine in position pTyr + 2 of the sequence. We have identified a suitable replacement for this residue.

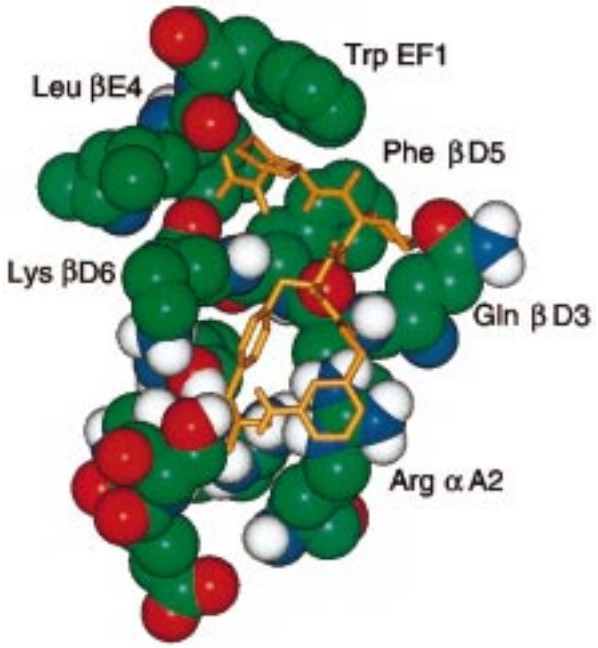

Figure 5. X-ray crystal structure of the Grb2-SH2 domain in complex with **2b** (yellow). Only the amino acid residues of the SH2 domain within a distance of 4 Å of the ligand are shown.

As shown by X-ray crystallography, the β-amino acid (amino protected), *cis*-2-amino-cyclohex-3-ene carboxylic acid, mimics the hydrogen bond interactions of asparagine with the SH2 domain in full agreement with our design. Thus with **2b**, we have obtained a high-affinity ligand of low molecular weight in which two of the three initial natural amino acids of the minimal sequence have been replaced by nonproteinogenic amino acids. Furthermore, our asparagine mimetic allows the elimination of one peptide bond (the C-terminal carboxamide group involved in the β-turn intramolecular hydrogen bond) compared to previously described compound **1**. Therefore, the work reported here constitutes a progress in our effort to identify an antagonist of the Grb2-SH2 domain suitable for pharmacological investigations.

Experimental Section

General. 4-(2′,4′-Dimethoxyphenyl-Fmoc-aminomethyl)-phenoxy-polystyrene resin (1% DVB cross-linked, 0.4 mequiv/g, 100−200 mesh) was purchased from NovaBiochem (Läufelfingen, Switzerland). TPTU reagent was from Senn Chemicals AG (Dielsdorf, Switzerland). HATU reagent was from PerSeptive Biosystems (Hamburg, Germany). The required Fmoc derivatives were obtained using standard protocols. N^a-Fmoc-Tyr(PO_3H_2)-OH was synthesized as described previously.[20] Trifluoroacetic acid, diisopropylethylamine, and piperidine were from Fluka (Buchs, Switzerland). *N*,*N*-Dimethylacetamide was from Merck (Hohenbrunn, Germany) and *N*-methylpyrrolidin-2-one was from SDS (Peypin, France). All commerical chemicals used were of the highest quality available (AR grade or higher). TLC was performed on precoted silica gel plates (60F-254, 0.2 mm thick, Merck); visualization was obtained by dipping the plates in a stainning solution (2.5 g of phosphormolybdic acid and 0.6 g of cerium(IV) sulfate in 1 L of 1 M H_2SO_4) following by heating the plates with an air gun. The melting points were determined on a Büchi 510 melting point instrument and are uncorrected. Silica gel column chromatography was carried out with Merck silica gel 60 (particle size 0.040−0.063 mm) at 0.5 bar. Peptide retention times (t_R) were measured by RP-HPLC on a Spectra-Physics

liquid chromatography system. Preparative purification was carried out on a Büchi system (Büchi 687 gradient former and Büchi 688 chromatography pump) using a C_{18}-column (Merck LICHROPREP RP-18, 15−25 μm bead diameter, reversed-phase HPLC column material based on C_{18}-derivatized silica gel, Merck, Darmstadt, FRG; column length 46 cm, diameter 3.6 cm; flow rate 53.3 mL/min; detection at 215 nm) eluted with an acetonitrile−water gradient containing 0.1% of TFA. NMR spectra of the compounds were recorded on a Varian Gemini-300, Bruker 250, or Bruker Avance-500 spectrometers. All ^{1}H NMR spectra are reported in δ units, ppm downfield from tetramethylsilane using the residual solvent signal as an internal standard. Coupling constants (J) are reported in hertz (Hz). Electrospray ionization mass spectra (ESI MS) were obtained with a Fisons Instruments VG Platform II. High-resolution mass spectra (HRMS) were recorded on a Micromass Quattro II instrument.

***rac,cis*-7-Azabicyclo[4.2.0]-oct-4-en-8-one (4).** A solution of cyclohexa-1,3-diene (27.5 mL, 0.29 mol) in dichloromethane (200 mL) was added to a solution of chlorosulfonyl isocyanate (25 mL, 0.29 mol) in dichloromethane (200 mL) over 10 min. After 30 min at room temperature, the reaction mixture was added to a stirred solution of potassium carbonate (84 g, 0.86 mol) and sodium sulfite (3.6 g 0.03 mol) in water (600 mL). Additional water (500 mL) was added to the mixture. The organic layer was separated, and the aqueous layer was extracted with ether (2 × 800 mL). The combined organic layer and extracts were washed with water (2 × 200 mL), dried over anhydrous magnesium sulfate, and evaporated to dryness under reduced pressure. Recrystallization from diisopropyl ether/*n*-hexane afforded pure compound **4** (12.2 g, 35%) as colorless crystals: mp 74−76 °C (lit.[16]mp 70.5−71.5 °C); ^{1}H NMR (250 MHz, $CDCl_3$) δ 5.9−6.2 (m, 3H), 4.05 (t, J = 4.8 Hz, 1H), 3.51 (m, 1H), 2.12 (m, 3H), 1.5−1.8 (m, 1H); ESI MS (positive ion mode) 124 $[M + H]^+$. Anal. (C_7H_9NO) C, H, N.

***rac,cis*-*N*-*tert*-Butoxycarbonyl-7-azabicyclo[4.2.0]-oct-4-en-8-one (5).** Triethylamine (6.8 mL, 49 mmol), di-*tert*-butyl dicarbonate (21.3 g, 97 mmol), and 4-(dimethylamino)pyridine (6.0 g, 49 mmol) were added to a solution of *rac*,*cis*-7-azabicyclo[4.2.0]-oct-4-en-8-one (6.0 g, 49 mmol) in dichloromethane (100 mL) under a nitrogen atmosphere. The reaction mixture was stirred for 6 h at room temperature and then poured into 2 M HCl (150 mL). The organic layer was separated, and the aqueous layer was extracted with dichloromethane (2 × 150 mL). The combined organic layer and extracts were washed with water (100 mL), dried over anhydrous magnesium sulfate, and evaporated to dryness under reduced pressure. The residue was purified by flash column chromatography on silica gel using ethyl acetate/*n*-hexane (1:4) to obtain **5** (8.9 g, 82%) as a yellow oil: ^{1}H NMR (250 MHz, $CDCl_3$) δ 6.15 (m, 2H), 4.31 (dd, J = 4.3 Hz, J = 4.2 Hz, 1H), 3.49 (m, 1H), 2.04−2.14 (m, 3H), 1.66−1.77 (m, 1H), 1.52 (s, 9H); ESI MS (positive ion mode) 224 $[M + H]^+$. Anal. ($C_{12}H_{17}NO_3$) calcd C, H, N.

***rac,cis*-2-(*tert*-Butoxycarbonylamino)-cyclohex-3-ene Carboxylic Acid (6).** A solution of lithium hydroxide monohydrate (4.1 g 97 mmol) in water (100 mL) was added to a stirred solution of *rac*,*cis*-*N*-*tert*-butoxycarbonyl-7-azabicyclo-[4.2.0]-oct-4-en-8-one (7.0 g; 31 mmol) in THF (140 mL). The reaction mixture was stirred for 7 h at room temperature. After this time, the THF was removed by evaporation, and the solution was acidified to pH 4 by adding 10% acetic acid. The mixture was extracted with ether (2 × 400 mL), dried over anhydrous magnesium sulfate, and evaporated to dryness under reduced pressure. The residue was recrystallized from ethyl acetate/*n*-hexane to afford pure **6** (6.9 g, 91%) as colorless crystals: mp 122−123 °C (lit.[21] mp 110−118 °C); ^{1}H NMR (250 MHz, DMSO-d_6) δ 11.72 (bs, 1H, COO*H*), 6.11 (bd, 1H, N*H*), 5.72 (m, 1H, *H*-olefin), 5.60 (m, 1H, *H*-olefin), 4.36 (m, 1H, C*H*(β)) 2.61 (m, 1H, C*H*(a)), 2.06−1.70 (m, 4H), 1.85−2.0, 1.38 (s, 9H, *t*-Bu); ESI MS (positive ion mode) 242 $[M + H]^+$. Anal. ($C_{12}H_{19}NO_4$) C, H, N.

***rac,cis*-2-(9-Fluorenylmethoxycarbonylamino)-cyclohex-3-ene Carboxylic Acid (3).** *rac*,*cis*-2-(*tert*-Butoxycarbonylamino)-cyclohex-3-ene carboxylic acid (2 g, 8.3 mmol) was added to a stirred solution of 4 N HCl in dioxane (20 mL). After 50 min at room temperature, the solution was concentrated to dryness and the residue was evaporated two times from petrolether to remove traces of HCl. The residue was triturated with cold ether, filtered, and dried overnight in a desiccator over NaOH pellets. The compound (0.6 g, 3.6 mmol) was dissolved in MeCN:H_2O (1:1, v/v; 12 mL) and stirred vigorously. To this stirred solution were added triethylamine (1.64 mL, 11.76 mmol) and fluorenylmethylsuccinimidyl carbonate (1.7 g, 5.03 mmol). After the mixture was stirred for 3 h, the acetonitrile was evaporated, water (20 mL) was added, and the suspension was extracted with ether (3 × 15 mL). The aqueous layer was acidified with 1 N HCl to pH 2−3, and the suspension was extracted with ethyl acetate (3 × 25 mL). The combined ethyl acetate extracts were washed with brine, dried over anhydrous magnesium sulfate, and evaporated to dryness under reduced pressure. The crude compound was purified by flash chromatogray on silica gel using dichloromethane/methanol to obtain the title compound (979 mg, 80%) as an oil. A sample was crystallized from chloroform/diisopropyl ether/petroleum ether: mp 128−130 °C; ^{1}H NMR (500 MHz, DMSO-d_6) δ 12.07 (bs, 1H, COO*H*), 7.88 (d, J = 7.6 Hz, 2H), 7.74 (d, J = 7.5 Hz, 1H), 7.69 (d, J = 7.5 Hz, 2H), 7.41 (dd, J = 7.5 Hz, 2H), 7.36 (d, J = 9.9 Hz, 1H, N*H*), 7.33 (m, 2H), 5.79 (m, 1H, *H*-olefin), 5.61 (m, 1H, *H*-olefin), 4.45 (m, 1H, C*H*(β)), 4.19 (m, 3H), 2.59 (m, 1H, C*H*(a)), 1.70−2.06 (m, 4H); ESI MS (positive ion mode) 386.2 $[M + Na]^+$. Anal. ($C_{22}H_{21}N_1O_4$) C, H, N.

Phosphopeptide Synthesis. The synthesis of peptide **1** was published previously.[8] Phosphopeptide **2** was synthesized manually on a 4-(2′,4′-dimethoxyphenyl-aminomethyl)-phenoxy resin, employing the fluorenylmethoxycarbonyl strategy. Fmoc removal was with piperidine/DMA (1:4, v/v; 6 × 2 min), followed by washing with MeOH (3 × 1 min), NMP (2 × 1 min), MeOH (3 × 1 min), and NMP (3 × 2 min). Coupling was achieved by first dissolving the Fmoc-amino acid (2 equiv), DIEA (5 equiv), and HATU or TPTU (2 equiv) in NMP, waiting 3 min for preactivation, adding the mixture to the resin, and finally shaking for at least 2 h. The incorporation of **1** and Fmoc-1-aminocyclohexyl carboxylic acid was accomplished with HATU (first coupling) and TPTU (second coupling) as described above. N^a-Fmoc-Tyr(PO_3H_2)-OH was coupled with TPTU (first coupling) and HATU (second coupling) as described above. 3-*N*-*tert*-Butoxycarbonyl-aminobenzyl-4-nitrophenyl-carbonate (3 equiv[8]) was coupled to the N-terminal residue of the peptide resin in the presence of an equimolar amount of DIEA in NMP during 17 h at room temperature. The complete peptide resin obtained after the last coupling step was simultaneosly deprotected and cleaved by treatment with 95% TFA/5% H_2O for 3 h at room temperature. The filtrate from the cleavage reaction was precipitated in diisopropyl ether/petroleum ether (1:1, v/v, 0 °C), and the precipitate collected by filtration. The crude peptide was purified by medium-pressure liquid chromatography using a C_{18}-column eluted with H_2O/0.1% TFA (buffer A) and MeCN/0.09% TFA (buffer B): 7 min with 100% buffer A, 7 min linear gradient from 0% to 10% buffer B, 30 min from 10% to 16% buffer B, 15 min from 16% to 18% buffer B, and 7 min from 18% to 19% buffer B; detection at 215 nm. A second purification was carried out to obtain pure peptide **2b**: 7 min with 100% buffer A, 10 min linear gradient from 0% to 13% buffer B, 30 min from 13% to 17% buffer B, 15 min from 17% to 18% buffer B, and 10 min from 18% to 19% buffer B; detection at 215 nm. Fractions shown by analytical HPLC to be >95% pure were pooled and lyophilized to provide the title compounds as white powder TFA salts: HRMS obs. 680.2452 (**2a**) $[M + Na]^+$, calcd for $C_{31}H_{39}N_5O_9P_1Na_1$ 680.2463; HRMS obs. 680.2456 (**2b**) $[M + Na]^+$, calcd for $C_{31}H_{39}N_5O_9P_1Na_1$ 680.2463. The purity of the peptides was verified by reversed-phase analytical HPLC on a Nucleosil C_{18}-column (250 × 4 mm, 5 μm, 100 Å): linear gradient over 10 min of MeCN/0.09% TFA and H_2O/0.1% TFA from 1:49 to 3:2, flow rate 2.0 mL/min, detection at 215 nm; single peak at t_R= 6.18 min (**2a**); t_R= 6.32 min (**2b**); ^{1}H NMR

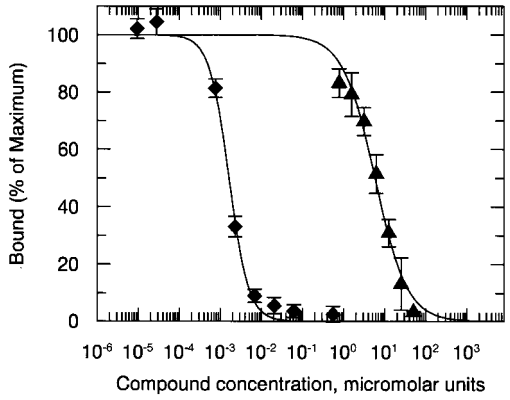

Figure 6. Inhibition curve of compound **2b** in the EGFR assay (◆) and that of the Ac-EpYINQ-NH2 phosphopeptide, IC_{50} = 5.8 ± 0.5 as control (▲). The standard deviation represents the mean of triplicates.

(500 MHz, 300 K, DMSO-d_6) of **2b** δ 7.82 (s, 1H, N*H*), 7.44 (d, J = 8.3 Hz, 1H, N*H*-urethane), 7.27 (d, J = 8.6 Hz, 2H, *H*-phenyl, pTyr), 7.23 (s, 1H, N*H*-carboxamide), 7.15 (d, J = 8.8 Hz, 1H, N^a*H*), 7.05 (d, J = 8.2 Hz, 2H, *H*-phenyl, pTyr), 7.01 (t, J = 7.5 Hz, 1H, *H*-benzyloxy), 6.77 (s, 1H, N*H*-carboxamide), 6.55 (m, 3H, *H*-benzyloxy), 5.68 (m, 1H, *H*-olefin), 5.49 (m, 1H, *H*-olefin), 4.81 (s, 2H, CH_2-benzyloxy) 4.49 (m, 1H, *H*-C(β)), 4.28 (m, 1, *H*-C(a), pTyr), 3.01 (dd, J = 13.5 Hz, J = 3.5 Hz, *H*-C(β), pTyr), 2.68 (dd, J = 13.5 Hz, J = 11.5 Hz, *H*-C(β), pTyr), 2.53 (m, 1H, *H*-C(a)), 1.12−2.09 (m, 14H).

Abbreviations. The abbreviations for amino acids and the nomenclature of peptide structures follow the recommendations of the IUPAC−IUB Commission on Biochemical Nomenclature (*Eur. J. Biochem*. **1984**, *138*, 9). Other abbreviations are as follows: Ac_6c, 1-aminocyclohexylcarboxylic acid; Boc, *tert*-butyloxycarbonyl; DCM, dichloromethane; DIEA, diisopropylethylamine; DMA, *N*,*N*-dimethylacetamide; DMAP, 4-(dimethylamino)pyridine; EGFR, epidermal growth factor receptor; ESI MS, electrospray ionization mass spectra; Fmoc, 9-fluorenylmethyloxycarbonyl; Grb2, growth factor receptor-bound protein 2; HATU, *N*-[(dimethylamino)-1*H*-1,2,3-triazolo-[4,5-*b*]pyridin-1-ylmethylene]-*N*-methylmethanaminium hexafluorophosphate *N*-oxide; HPLC, high-performance liquid chromatography; HRMS, high-resolution mass spectra; MBHA, methoxybenzhydrylamine; MPLC, medium-pressure liquid chromatography; NMR, nuclear magnetic resonance; NMP, *N*-methylpyrrolidin-2-one; SH2, Src homology 2; TEA, triethylamine; TFA, trifluoroacetic acid; THF, tetrahydrofuran; TLC, thin-layer chromatography; TPTU, 2-(2-oxo-1(2H)-pyridyl)-1,1,3,3-tetramethyluronium tetrafluoroborate; t_R, retention time.

EGFR Assay. The EGFR assay has already been described in detail previously.[10] Briefly, phosphorylated MBP-EGFR immobilized on a solid phase (polystyrene microtiter plates, NUNC MAXYSORB) was incubated with a GST/Grb2-SH2 fusion protein capable of binding to it, in the presence of phosphopeptide in buffer or buffer alone. Bound SH2 was detected with polyclonal rabbit anti-GST antibody. Following washing, horseradish peroxidase-conjugated mouse anti-rabbit antibody was added. Peroxidase activity is monitored at 655 nm on a plate reader by adding 100 μL/well of a solution of tetramethylbenzidine as substrate.

Data Analysis. Compound inhibition was calculated as a percentage of the reduction in absorbance in the presence of each inhibitor concentration compared to the absorbance obtained with GST/SH2 in the absence of inhibitor. Dose−response relationships were constructed by nonlinear regression of the competition curves with Grafit (Erithacus Software, London, U.K.). Fifty percent inhibitory concentrations (IC_{50}) were calculated from the regression lines (Figure 6).

X-ray Crystallography. Cloning and expression of the Grb2 SH2 domain have been described earlier.[10] A solution of pure protein (Grb2 55−153) was concentrated with a Centricon (Amicon Grace Company) to 10−10.4 mg/mL and mixed with a 5-fold molar excess of **2b**. Small crystals of the complex with **2b** were obtained after a few days in 0.1 M HEPES, pH 7.5, and 1.4 M sodium acetate by the hanging drop vapor diffusion method. The crystals belong to the orthorhombic space group $P2_12_12_1$ with lattice constants 73.8 × 93.3 × 232.8 Å and diffract to 3.0 Å resolution.

One of these crystals (0.1 × 0.1 × 0.05 mm^3) was cryocooled at 100 K, and data were collected at this temperature on a MAR area detector mounted on an FR591 rotating anode X-ray generator (Enraf-Nonius) operating at 4.1 kW and producing graphite monochromated Cu Kα radiation. Frames (exposure: 25 min, crystal rotation: 0.5°) were processed using the MARXDS and the MARSCALE software programs.[22] The R_{merge} for all data between 30.0 and 3.0 Å is 20% with a 3.9-fold redundancy. The overall completeness of the data is 96%, and the same for data in the shell between 3.5 and 3.0 Å.

The large crystal unit cell (1.6 × 10^6 Å^3) indicates the presence of many molecules of the complex in the asymmetric unit (V_m = 2.9 Å^3/Da of protein for 12 protein molecules). A model comprising a dimer of the protein, which has been observed in the five different crystal forms obtained so far in our laboratory, was used as a probe for molecular replacement with the program AMORE.[23] The highest 10 peaks obtained in the rotation function were applied in the translation function. Due to the weakness of the data it was not possible to define unambiguously to which orthorhombic space group the crystal belongs to. The translation function had to be repeated in the four possible space groups ($P222$, $P222_1$, $P2_12_12$, and $P2_12_12_1$) plus the four axis permutations in space groups $P222_1$ and $P2_12_12$. Only the space group $P2_12_12_1$ gave acceptable results in the calculation of the translation function, giving a strong indication that it was the correct space group. Nevertheless, the peak obtained for the first dimer was not completely convincing (correlation factor = 0.249, R_{factor} = 0.493). In the course of iteration of the translation function with additional dimers, the correlation factor increased constantly while the R_{factor} decreased considerably. After the introduction of six dimers in the model the correlation factor was 0.642 and the R_{factor} 0.369. Visual inspection confirmed that the resulting packing in the crystal cell unit was reasonable.

The refinement was performed with the program XPLOR,[24] and manual rebuilding of the models was performed with the program O.[25] All data between 30.0 and 3.0 Å were used, and a bulk solvent correction was applied. A first cycle of rigid body refinement was performed to position the 12 molecules

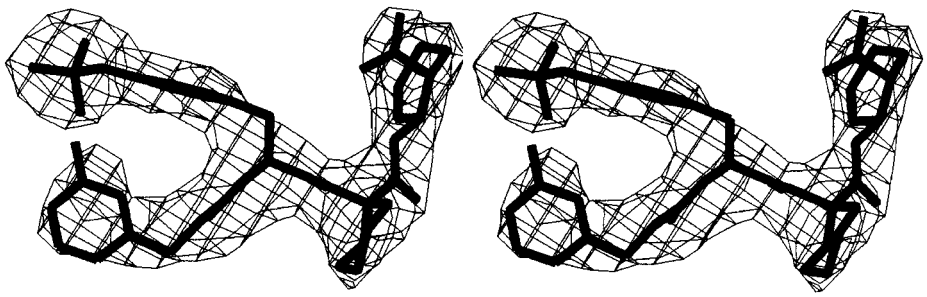

Figure 7. Stereoview of an $F_{obs}-F_{calc}$ electron density map in the binding site of Grb2-SH2 after refinement. The inhibitor which has been omitted from F_{calc} is represented. The electron density is contoured at 3 σ above the mean density.

more precisely. The second step consisted of refinement of the protein alone using strict noncrystallographic symmetry. Visual inspection of an electron density map confirmed the presence of the ligand in the active site and allowed its complete insertion into the model. Further refinement was performed, followed by minor modifications of the protein and addition of two solvent molecules per protein monomer. The final model consists of 96 protein residues, 53 inhibitor atoms, and 4 water molecules. The R_{factor} (R_{free}) dropped to 0.305 (0.318) with acceptable deviations of ideal geometry (rms deviation 0.027 Å and 2.536° for bonds and bond angles, respectively). Analysis of main chain torsion angles using PROCHECK[26] showed that 86% of the residues are located in the most favored regions, the remaining 14% occurring in the additional allowed regions of the Ramachandran plot. All the atoms of the inhibitor have been located within the electron density (Figure 7).

The coordinates of the X-ray structure have been deposited in the Brookhaven Protein Data Bank with accession code 1CJ1 for immediate availability.

Molecular Modeling. The modeling work was performed in MacroModel v.4.0[27] ("in house" version enhanced for graphics by A. Dietrich, unpublished results). Energy minimizations were performed using the AMBER force field[28] in conjunction with the GB/SA water solvation model.[29] The conformation of *cis*-Achec necessary to mimic the asparagine of **1 (**shown in Figure 3) is of low energy (within 1 kcal/mol of the calculated global minimum). The two-dimensional query shown in Figure 2 and the subsequent substructure search were made using the ISIS DRAW-ISIS BASE software, version 2.1.3d (MDL). The full Novartis corporate database of compounds was searched. The search gave 10 hits from which *cis*-Achec was selected as an available and rigid building block.

Acknowledgment. We thank R. Wille, D. Arz, V. von Arx, and C. Stamm for their technical assistance.

References

(1) Chardin, P.; Cussac, D.; Maigan, S.; Ducruix, A. The Grb2 Adaptor. *FEBS Lett.* **1995**, *369*, 47−51.
(2) Downward, J. The Grb2/Sem-5 Adaptor Protein. *FEBS Lett.* **1994**, *338*, 113−117.
(3) Lowenstein, E. J.; Daly, R. J.; Batzer, W. L.; Margolis, B.; Lammers, R.; Ullrich, A.; Skolnik, E. Y.; Bar-Sagi, D.; Schlessinger, J. The SH2 and SH3 Domain-Containing Protein Grb2 Links Receptor Tyrosine Kinases to ras Signaling. *Cell* **1992**, *70*, 431−442.
(4) Gishizky, M. L. Tyrosine Kinase Induced Mitogenesis Breaking the Link with Cancer. In *Annual Reports in Medicinal Chemistry*; Bristol, J. A., Ed; Academic Press: San Diego, 1995; Vol. 30, pp 247−253.
(5) Smithgall, T. E. SH2 and SH3 Domains: Potential Targets for Anti-Cancer Drug Design. *J. Pharmacol. Toxicol. Methods* **1995**, *34*, 125−132.
(6) Beattie, J. SH2 Domain Protein Interaction and Possibilities for Pharmacological Intervention. *Cell Signal.* **1996**, *2*, 75−86.
(7) Furet, P.; Gay, B.; Garcia-Echeverria, C.; Rahuel, J.; Fretz, H.; Schoepfer, J.; Caravatti, G. Discovery of 3-Aminobenzyloxycarbonyl as an *N*-Terminal Group Conferring High Affinity to the Minimal Phosphopeptide Sequence Recognized by the Grb2-SH2 Domain. *J. Med. Chem.* **1997**, *40*, 3551−3556.
(8) Garcia-Echeverria, C.; Furet, P.; Gay, B.; Fretz, H.; Rahuel, J.; Schoepfer, J.; Caravatti, G. Potent Antagonists of the SH2 Domain of Gbr2: Optimization of the X_{+1} position of 3-amino-Z-Tyr(PO_3H_2)-X_{+1}-Asn-NH_2. *J. Med. Chem.* **1998**, *41*, 1741−1744.
(9) Furet, P.; Gay, B.; Caravatti, G.; Garcia-Echeverria, C.; Rahuel, J.; Schoepfer, J.; Fretz, H. Structure-Based Design and Synthesis of High Affinity Tripeptide Ligands of the Grb2-SH2 Domain. *J. Med. Chem.* **1998**, *41*, 3442−3449.
(10) Rahuel, J.; Gay, B.; Erdmann, D.; Strauss, A.; Garcia-Echeverria, C.; Furet, P.; Caravatti, G.; Fretz, H.; Schoepfer, J.; Gruetter, M. Structural Basis for Specificity of Grb2-SH2 Revealed by a Novel Ligand Binding Mode. *Nature Struct. Biol.* **1996**, *3*, 586−589.
(11) Ligand residues are numbered relative to the position of the phosphotyrosine which is denoted pTyr 0.
(12) Songyang, Z.; Shoelson, S. E.; McGlade, J.; Olivier, P.; Pawson, T.; Bustelo, X. R.; Barbacid, M.; Sabe, H.; Hanafusa, H.; Yi. T.; Ren, R.; Baltimore, D.; Ratnofsky, S.; Feldman, R. A.; Cantley, L. C. Specific Motifs Recognized by the SH2 Domains of Csk, 3BP2, fps/fes, GRB-2, HCP, SHC, Syk and Vav. *Mol. Cell. Biol.* **1994**, *14*, 2777−2785.
(13) Songyang, Z.; Shoelson, S. E.; Chaudhuri, M.; Gish, G.; Pawson, T.; Hase, W. G.; King, F.; Roberts, T.; Ratnofsky, S.; Lechleider, R. J.; Neel, B. G.; Birge, R. B.; Fajardo, J. E.; Chou, M. M.; Hanafusa, H.; Schaffhausen, B.; Cantley, L. C. SH2 Domains Recognize Specific Phosphopeptide Sequences. *Cell* **1993**, *72*, 767−778.
(14) For the nomenclature of the SH2 domain residues see: Lee, C. H.; Kominos, D.; Jacques, S.; Margolis, B.; Schlessinger, J.; Shoelson, S. E.; Kuriyan, J. Crystal Structures of Peptide Complexes of the Amino-Terminal SH2 Domain of the Syp Tyrosine Phosphatase. *Structure* **1994**, *2*, 423−438.
(15) 3-amino-Z-pTyr-Ac_6c-βAla-NH2 has an activity in the micromolar range in the EGFR assay (Garcia-Echeverria, C.; et al. Novartis Pharma Inc., Oncology Research Department, unpublished results).
(16) Malpass, J. R.; Tweddle, N. J. Reaction of Chlorosulphonyl Isocyanate with 1,3-Dienes. Control of 1,2- and 1,4-Addition Pathways and the Synthesis of Aza- and Oxa-bicyclic Systems. *J. Chem. Soc., Perkin Trans. I* **1977**, 874−884.
(17) Durst, T.; O'Sullivan, M. J. Reduction of *N*-Chlorosulfonyl β-Lactams to β-Lactams with Sodium Sulfite. *J. Org. Chem.* **1970**, *35*, 2043−2045.
(18) Rink, H. Solid-phase Synthesis of Protected Peptide Fragments Using a Trialkoxy-Diphenyl-Methyl Ester Resin. *Tetrahedron Lett.* **1987**, *28*, 3787−3790.
(19) Atherton, E.; Sheppard, R. C. In *Solid-Phase Peptide Synthesis − A Practical Approach*; Richwood, D., Hames, B. D., Eds.; IRL Press at Oxford University Press: Oxford, 1989.
(20) Ottinger, E. A.; Shekels, L. L.; Bernlohr, D. A.; Barany, G. Synthesis of Phosphotyrosine-Containing Peptides as Their Use as Substrates for Protein Tyrosine Phosphatases. *Biochemistry* **1993**, *32*, 4354−4361.
(21) Bayer AG, EP 376072, 1990.
(22) Kabsch, W. Evaluation of a Single-Crystal Diffraction Form a Position-Sensitive Detector. *J. Appl. Crystallogr.* **1988**, *21*, 916−624.
(23) Navaza, J. AMORE: An Automated Package for Molecular Replacement. *Acta. Crystallogr.* **1994**, *D50*, 157−163.
(24) Brünger, A. T. *X-PLOR Version 3.1: A System for X-ray Crystallography and NMR*; Yale University Press: New Haven and London, 1992.
(25) Jones, A. T.; Zou, J.-Y.; Cowan, S. W.; Kjeldgaard, M. Improved Methods for Building Protein Models in Electron Density Maps and the Location of Errors in these Models. *Acta Crystallogr.* **1991**, *A47*, 110−119.
(26) Laskowski, R. A.; MacArthur, M. W.; Moss, D. S.; Thornton, J. M. PROCHECK: A Program to Check the Stereochemical Quality of Protein Structures. *J. Appl. Crystallogr.* **1993**, *26*, 283−291.
(27) Mohamadi, F.; Richards, N. G.; Guida, W. C.; Liskamp, R.; Lipton, M.; Caufield, C.; Chang, G.; Hendrickson, T.; Still, W. C. Macromodel- An Integrated Software System for Modeling Organic and Bioorganic Molecules Using Molecular Mechanics. *J. Comput. Chem.* **1990**, *11*, 440−467.
(28) Weiner, S. J.; Kollman, P.; Case, D. A.; Singh, U. C.; Ghio, C.; Alagona, S.; Profeta, S.; Weiner, P. A Force Field for the Simulation of Nucleic Acids and Proteins. *J. Am. Chem. Soc.* **1984**, *106*, 765−770.
(29) Still, W. C.; Tempczyk, A.; Hawley, R. C.; Hendrickson, T. Semianalytical Treatment of Solvation for Molecular Mechanics and Dynamics. *J. Am. Chem. Soc.* **1990**, *112*, 6127−6129.

JM991013U